MODELING THE SEPARATION FLOW AROUND A CYLINDER NEAR A SCREEN

S. M. Belotserkovskii, V. N. Kotovskii,
M. I. Nisht, and R. M. Fedorov

UDC 533.695.5

The nonstationary separation flow of an incompressible viscous fluid around a circular cylinder at different distances from a plane screen is investigated in a numerical experiment.

The distinguishing singularity of the flow around a cylinder at a screen is, as has been established by experimental investigations [1, 2], the appearance of a force repelling it from the screen. The origination of repulsive aerodynamic forces has also been detected in certain theoretical and experimental researches ([3, 4], say) in which the flow around two circular series arranged side-by-side was studied. At the same time, the interaction between streamlined bodies (for instance, ship hulls in a reservoir) causes them to attract each other.

On the basis of a theoretical approach proposed in [5, 6] and used to investigate the flow around vibrating and rotating cylinders [7, 8], the nonstationary separation flow around a circular cylinder at different distances from a screen is studied in a numerical experiment in this paper.

The separation flow around a cylinder at a screen was modeled by using the main and the specularly mapped vortex systems. Both the main and the specularly mapped vortex systems consist of total discrete vortices Γ_+ located directly at the cylinder surface, and free discrete vortices Δ_i ($i = 1, 2, \ldots$) of the aerodynamic wave (Fig. 1). The circulations of the corresponding discrete vortices of these systems are equal in magnitude and opposite in sign. The motion of the free discrete vortices occurs symmetrically relative to the line of symmetry of both vortex systems. In such diagramming of the flow, the condition of nonpenetration at any time is satisfied automatically on this line, which is equivalent to the presence of a plane screen of infinite length.

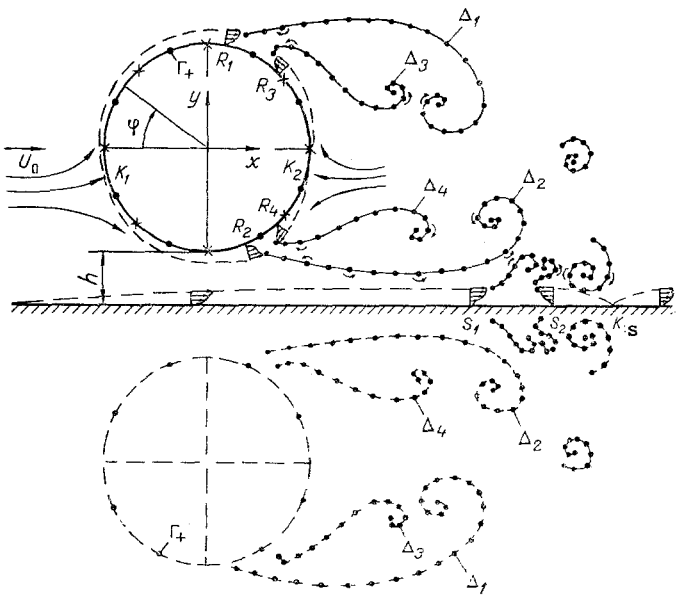

Fig. 1. Computational diagram.

Translated from Inzhenerno-Fizicheskii Zhurnal, Vol. 50, No. 2, pp. 188-195, February, 1986. Original article submitted January 14, 1985.

0022-0841/86/5002-0129$12.50

The system of linear algebraic equations to determine the circulations of the attached discrete vortices has the form

$$\sum_{\mu=1}^{N} \Gamma_\mu^r [w_{x\mu\nu} \cos(n,\ x) + w_{y\mu\nu} \cos(n,\ y)] + C = -\cos(n,\ x) -$$

$$- \sum_{i=1}^{L} \delta_i [w_{xi\nu} \cos(n,\ x) + w_{yi\nu} \cos(n,\ y)],\ \nu = 1,\ 2,\ \ldots,\ N,$$

$$\sum_{\mu=1}^{N} \Gamma_\mu^r = F - \sum_{i=1}^{L} \delta_i. \qquad (1)$$

The dimensionless functions w_x and w_y in this system are calculated with the presence of the discrete vortices of the specularly mapped vortex system taken into account by means of the formulas $w_x = w_x(\bar{x}_\nu,\ \bar{y}_\nu,\ \bar{x}_p,\ \bar{y}_p) - w_x(\bar{x}'_\nu,\ \bar{y}'_\nu,\ \bar{x}_p,\ \bar{y}_p)$, $w_y = w_y(\bar{x}_\nu,\ \bar{y}_\nu,\ \bar{x}_p,\ \bar{y}_p) - w_y(\bar{x}'_\nu,\ \bar{y}'_\nu,\ \bar{x}_p,\ \bar{y}_p)$, where $\bar{x}_p$, $\bar{y}_p$ are the dimensionaless coordinates of the points at which the velocity is calculated, $\bar{x}_\nu$, $\bar{y}_\nu$ and $\bar{x}'_\nu$, $\bar{y}'_p$ are the dimensionless coordinates of a discrete vortex of the main system and its corresponding vortex of the specularly mapped vortex system [9], L is the quantity of free discrete vortices in the aerodynamic wake of the cylinder at a given time, and F is a constant determined by the initial conditions of the problem. If the motion starts from a state of rest, then F = 0.

The first N equations of the system (1) are the impenetrability conditions at N check points located on the cylinder surface between the discrete vortices, and the last equation is the Thomson theorem about the constancy of circulation within a closed contour enclosing the cylinder and its aerodynamic wave.

Since the system (1) is overdefined, then the regularizing variable C that results in cancellation of the mentioned overdefinition [10] is introduced.

The system (1) is solved in combination with the solution of the problem of a viscous flow in a boundary layer [5, 6] and determines the stream parameters at any point of the flow plane since its velocity components at this point can be calculated from the formulas

$$V_x = 1 + \sum_{\mu=1}^{N} \Gamma_\mu^r\, w_{x\mu} + \sum_{i=1}^{L} \delta_i w_{xi},\ V_y = \sum_{\mu=1}^{N} \Gamma_\mu^r\, w_{y\mu} + \sum_{i=1}^{L} \delta_i w_{yi}.$$

The stream velocity is $V = V_x \cos(n, y) - V_y \cos(n, x) + \gamma/2$ on the cylinder surface. By realizing the solution of the problem under consideration at each rated time, the process of the origination, formation, and development of separation flow around a cylinder near a screen can be studied.

As usual, the viscous flow in the boundary layer on a cylinder is computed by means of the velocity distribution found on its surface from the forward stagnation point K_1 to its separation points R_1 and R_2 (Fig. 1), which are determined from the condition $\partial u/\partial n \to 0$ on the cylinder surface at these points.

Upon origination of a reverse flow with the formation of second and more stagnation points, the boundary layer from these points to the corresponding separation points is also computed. The value of the boundary layer parameters at its points of separation determines the magnitude of the circulation and the direction of motion in the first time step after separation of the discrete vortices of the free vortex sheets that model the boundary layer being separated at these points [5, 6] from the cylinder.

The boundary layer being developed along the screen exerts influence on the flow in the gap between the cylinder and screen. This influence can be especially substantial at low Re numbers and small gaps because of the displacing action of the boundary layer of both the cylinder and the screen.

The boundary layer on the screen is computed from its beginning, which is given at that distance from the cylinder at which the flow is practically undisturbed. As usual, the boundary conditions for its analysis are the conditions for stream particle attachment to the

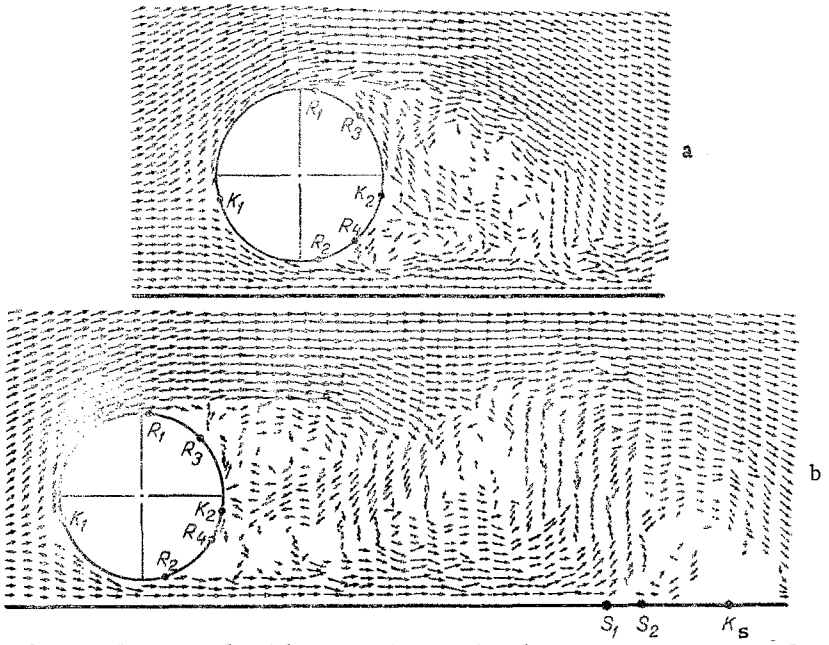

Fig. 2. Velocity field around a cylinder near a screen for $Re = 0.6 \cdot 10^6$; a) $\bar{h} = 0.2$; $\tau = 3.2$; b) $\bar{h} = 0.13$; $\tau = 7.5$ (all quantities dimensionless (b/r)).

screen surface and the tendency of the longitudinal velocity in the boundary layer towards the stream velocity in the nonviscous flow domain determined from the solution of the problem of the combined flow around the cylinder and screen. The velocity distribution for self-similar flow in the boundary layer on a flat plate [11] is used as the initial longitudinal and transverse velocity profiles in the boundary layer at the beginning of a screen. Later the flow along the screen which occurs under the effect of an external pressure gradient due to the hydrodynamic interaction between the cylinder and the screen is calculated by numerical integration of the system of nonstationary boundary layer differential equations.

Such flow regimes can occur in the combined flow around a cylinder and screen when the boundary layer will also be separated from the screen surface. In such cases, the free vortex sheets modeling the boundary layer being separated from the screen should additionally be included in the total computation scheme.

The velocity fields in the aerodynamic wake behind the cylinder for a flow with number $Re = 0.6 \cdot 10^6$ and different relative distances $\bar{h}$ between the cylinder and screen are presented in Fig. 2 at different times after the beginning of the motion.

The velocity field displayed in Fig. 2a corresponds to the dimensionless time $\tau = 3.2$ from the beginning of the motion for $\bar{h} = 0.2$. It is seen that the flow is retarded significantly in the domain between the lower frontal part of the cylinder and the screen, while the forward stagnation K_1 is shifted downward. This same regularity is also observed for other relative distances (for example, $\bar{h} = 0.13$, Fig. 2b), where the shift of the stagnation point mentioned to the lower cylinder surface is magnified as $\bar{h}$ diminishes.

Upon the origination of a reverse flow with the formation of two or several stagnation points in the cylinder base region, their location is unstable in time as for flow without a screen. However, as computations showed, upon the origination of two stagnation points on the cylinder surface, the rear stagnation point K_2 is on the lower surface a major part of the time.

A "slot" effect resulting in screen acceleration is observed in the domain of the minimal gap between the cylinder and screen. But this section has a moderate extent directly on the cylinder surface, including a part of its surface in an approximately 30° sector.

The flow around the cylinder at the upper frontal part occurs with significant stream acceleration. This is explained by the fact that the fluid mass flow through is slight for a small relative gap. Consequently, the cylinder and screen are flowed around as a certain

fictitious body with maximal thickening at the site of cylinder location. This indeed results in stream acceleration at the upper part of the cylinder.

The shift of the critical points and their associated elevated pressure zones to the lower cylinder surface and the stream acceleration with the formation of a rarefaction zone of significant extent on its upper frontal surface result in the cylinder lift at the screen being positive for all $\bar{h}$ despite the existence of a rarefaction zone of moderate extent on its surface in the neighborhood of the minimal gap with the screen.

In contrast to the considered nature of the flow around a cylinder near a screen on prolate streamlined bodies, for instance, profiles, at the screen, an attractive rather than a repulsive force occurs as computations show. This is associated with the fact that the stream converges with the thin trailing edge in direct proximity to this edge, and the displacement of the forward stagnation point because of the influence of the screen is not large. Consequently, a flow with large rarefraction is realized on the major point of the profile surface closest to the screen, and results in the formation of a negative lift.

In contrast to an isolated cylinder, the vortex structures behind a cylinder at a screen immediately are of nonsymmetric nature. As is seen from Fig. 2a, two nonsymmetric vortex bunches are formed behind the cylinder at the time $\tau = 3.2$, where the upper vortex bunch is of more regular shape and greater size than the lower. This is associated with the presence of the "slot" effect at the site of the minimal gap between the cylinder and the screen, which results in the stream at the screen surface directly behind the cylinder in the layer with thickness commensurate with the gap size being of considerably higher velocity. Consequently, the free discrete vortices being separated from the cylinder lower surfaces are entrained from the bottom domain of the lower part of the cylinder upon being incident in this layer, and thus hinders the formation of a powerful vortex bunch here. Since the total circulation of the discrete vortices that converge with the lower surface at the separation points R_2 and R_4 is negative, then by moving a distance approximately equal to the gap magnitude along the screen, they later induce a velocity that is in agreement with the direction of the free stream velocity. This contributes to conservation of the relatively high velocity level in the thin layer abutting on the screen that was mentioned earlier. The stream motion near the screen that has a greater velocity than in the central part of the aerodynamic wake results in the formation of a rarefaction that, as is seen from Figs. 2a and b, causes the attraction of vortex branches of the near aerodynamic wake to it.

The approach of the upper vortex bunch with positive circulation to the screen in the far aerodynamic wake can result in stream deceleration with the formation of the stagnation point K_e (Fig. 2b). The sufficiently high positive pressure gradient that occurs here and acts on the flow in the screen boundary layer causes the separations at the points S_1 and S_2 (Fig. 1).

On the whole, the far aerodynamic wake behind the cylinder at the screen has no such ordered structure with periodic arrangement of vortex bunches as is behind an isolated cylinder [6]. Here vortex bunches with positive circulation direction predominate, that have separated from the upper part of the cylinder, while the lower vortices dissociate mainly into finer vortex formation. The interface analogously influences the vortex wake in separation flow around a thin profile [9].

Represented in Fig. 3 are the change with time of the cylinder aerodynamic characteristics, the angular location of the forward stagnation point, and the boundary layer separation points for a relative distance of $\bar{h} = 0.13$ from the screen.

The singularity of the flow around a cylinder near a screen that the location of the boundary layer separation point R_1 from the upper frontal surface of the cylinder characterized by the angle ϕ_1 and is sufficiently stable (Fig. 3a). The location of the point R_2 of boundary layer separation from the lower frontal part of the cylinder also changes slightly. This is explained by the action of the screen on the aerodynamic wake, which reduces the transverse motion of the vortex bunches in the direct proximity to the cylinder and stabilizes the points of separation R_1 and R_2. The location of the separation points R_3 and R_4, on the other hand, is unstable. As for the isolated cylinder, this is associated with the intensive stream fluctuations on this part of the surface because of the influence of the closely located aerodynamic wake.

As an analysis of the velocity fields shows (see Fig. 2, say), the stream separates from the cylinder surface at points located between the boundary layer separation points

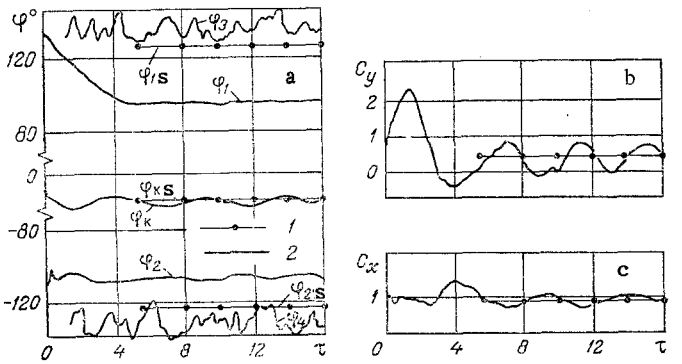

Fig. 3. Change in the angular location of the separation points $\phi_{1,2...}$ and the forward stagnation point Φ_k (deg) (a), lift coefficient C_y (b/r) (b) and frontal drag C_x (b/r) (c) in the time τ (b/r): 1) experimental data from [1, 2]; 2) computation.

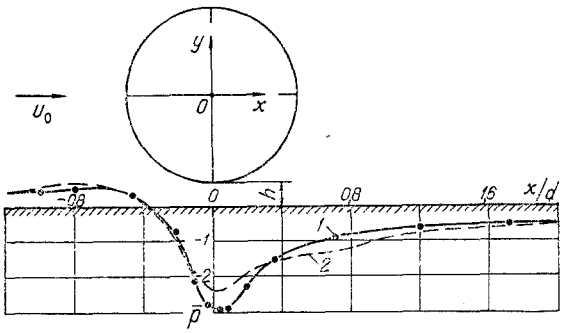

Fig. 4. Distribution of the pressure coefficient $\bar{p}$ (b/r) along the screen: 1) experimental data from [2]; 2) computation.

R_1 and R_3 on its upper surface and the points R_2 and R_4 on its lower surface. If points located midway between the mentioned boundary layer separation points are taken as the site of stream separation from the cylinder surface, then their location is in satisfactory agreement with the experimentally determined location of the stream separation points ϕ_{1e} and ϕ_{2e}, respectively [2].

The forward stagnation point K_1 is located on the lower surface of the frontal part of the cylidner at all times and its location is in good agreement with the experimental value of ϕ_{ke}. As the distance between the cylinder and screen increases, it shifts in the direction of its upper surface since the influence of the screen on the flow around the cylinder attenuates.

A singularity of the separation flow around a cylinder near a screen is also the fact that if the boundary layer separation points R_1 and R_2 do not change location in practice because of the periodic shedding of vortex bunches that cause rearrangement of the whole flow, then noticeable fluctuations are observed in the location of the forward stagnation point.

The cylinder lift and drag fluctuate also because of the fluctuations in the forward and rear stagnation points (Figs. 3b and c). The mean value of the lift with respect to time is positive and exactly as the mean value of the drag in completely satisfactory agreement with the experimental data.

The lift is reduced as the distance between the screen and cylinder increases, because of displacement of the forward stagnation point K_1, meaning the elevated pressure zone in the direction to the upper surface. This results in a diminution of the magnitude of the rarefaction and the rarefaction zone size on the upper frontal part of the cylinder.

The presence of a closely located screen has weak influence on the aerodynamic Strouhal number determined by the frequency of vortex bunch separation. The approach of the cylinder to the screen results in its certain growth from the value Sh = 0.18-0.20 for an isolated cylinder to the value Sh = 0.20-0.22 for the cylinder located closely to the screen.

The pressure distribution over the screen surface is shown in Fig. 4. It is seen that a positive pressure is ahead of the cylinder on a certain section of the screen surface because of deceleration of the stream by the cylinder. At the site where the transfer section of the channel between the cylinder and screen becomes narrow, a rarefaction occurs that reaches the maximal value somewhat further downstream than the site of minimal gap location between the cylinder surface and the screen. A satisfactory agreement between the computed and experimental data is also observed here.

It is characteristic that, as has been mentioned above, the rarefaction zone is conserved at a sufficiently large distance from the cylinder because of the singularities in the aerodynamic wake behind the cylinder. This is also the reason why the near aerodynamic wake seems to be attracted to the screen.

NOTATION

x, y, Cartesian coordinates; n, normal direction to the cylinder surface; d, cylinder diameter; h, distance between the cylinder and the screen; ϕ, angular location of boundary layer separation points and stagnation points; U_0, free stream velocity; W, perturbed velocity; V, stream velocity, u, longitudinal velocity in the boundary layer; γ, total attached vortex layer intensity; ν, kinematic viscosity; t, time; f, frequency of vortex bunch separation from the cylinder; Γ_+, Δ, circulation of the attached and free discrete vortices, respectively; C_y, C_x, lift and frontal drag coefficients, respectively; $Re = U_0 d/\nu$, Reynolds number; $\tau = tU_0/d$, dimensionless time; $Sh = fd/U_0$, Strouhal number; h, relative disance from the screen; p, pressure coefficient; $\Gamma = \Gamma_+/(U_0 d)$, $\delta = \Delta/(U_0 d)$, dimensionless circulations. Subscripts: r, computed time; the prime signifies parameters of the mapped vortex system; s, conditions on the screen; 0, at infinity ahead of the cylinder; and +, a dimensional quantity.

LITERATURE CITED

1. V. M. Kovalenko, N. M. Bychkov, G. A. Kisel', and N. D. Dikovaskaya, Flow around Rotating and Fixed Circular Cylinders near a Plane Screen, pp. 50-59 [in Russian], Reports 1, Nauka, Novosibirsk (1983).
2. V. M. Kovalenko, N. M. Bychkov, G. A. Kisel', and N. D. Dikovskaya, Flow around Rotating and Fixed Circular Cylinders near a Plane Screen [in Russian], Report 2, Nauka, Novosibirsk (1984), pp. 78-88.
3. V. E. Saren, "System of smooth profiles in a potential incompressible fluid flow," Dynamics of Continuous Media [in Russian], No. 22, pp. 43-48. Inst. Hydrodynamics Siberian Branch USSR Acad. Sciences (1975), pp. 43-48.
4. V. M. Bozhkov, L. E. Vasil'ev, and S. V. Zhigulev, "Singularities of transverse subsonic flow around a circular cylinder," Izv. Akad. Nauk SSSR, Mekh. Zhidk. Gaza, No. 2, 58-65 (1980).
5. V. N. Kotovskii, M. I. Nisht, and R. M. Fedorov, "Mathematical modeling of nonstationary separation flow around a cascade of solid profiles," Dokl. akad. Nauk SSSR, 263, No. 6, 1326-1330 (1982).
6. S. M. Belotserkovskii, V. N. Kotovskii, M. I. Nisht, and R. M. Fedorov, "Mathematical modeling of nonstationary separation flow around a circular cylinder," Izv. Akad. Nauk SSSR, Mekh. Zhidk. Gaza, No. 4, 138-147 (1983).
7. S. M. Belotserkovskii, V. N. Kotovskii, M. I. Nisht, and R. M. Fedorov, "Electrical computer study of singularities of separation flow around a vibrating cylinder," Inzh.-Fiz. Zh., 47, No. 1, 41-47 (1984).
8. S. M. Belotserkovskii, V. N. Kotovskii, M. I. Nisht, and R. M. Fedorov. "Electronic computer modeling of the separation flow around a rotating cylidner and reverse Magnus force," Inzh.-Fiz. Zh., 48, No. 2, 244-250 (1985).
9. S. M. Belotserkovskii and M. I. Nisht, Separated and Unseparated Flow around Thin Wings by an Ideal Fluid [in Russian], Nauka, Moscow (1978).
10. I. K. Lifanov, "On singular integral equations with one-dimensional and multiple Cauchy-type integrals," Dokl. Akad. Nauk SSSR, 239, No. 2, 265-268 (1978).
11. H. Schlichting, Boundary Layer Theory, McGraw-Hill (1968).